ESTIMATING EVAPOTRANSPIRATION IN THE SAHEL USING REMOTE SENSING PRODUCTS

J13.3

Mónica García [1,2,*], Inge Sandholt [1,2], Pietro Ceccato[2], Eric Mougin[3], Laurent Kergoat[3], Franck Timouk[3]

[1]Department of Geography & Geology, University of Copenhagen, Denmark
[2]International Research Institute for Climate & Society, The Earth Institute at Columbia University, New York, USA.
[3] Géosciences Environnement Toulouse (GET). Observatoire Midi-Pyrénées, 31400 Toulouse, France

ABSTRACT

Making available regional estimates of daily evapotranspiration in water-scarce and climatic vulnerable regions is critical for improving agricultural and hydrological information as well as our understanding of land surface-atmosphere interactions. The aim of this study is to provide an operational algorithm for the Sahel relying on satellite products at 1-4 km spatial resolution without field calibration. An evapotranspiration model based on the Priestley-Taylor equation reduced according to multiple stresses based on Fisher´s model was evaluated in a savanna site in the Sahel (Mali) introducing a new formulation for the soil moisture constraint. The model was successful to estimate daily evapotranspiration at the field level, with a better performance when using a soil moisture constraint based on a Thermal Inertia index (r^2=0.83; MAE=19.2 Wm^{-2}) than on an atmospheric water deficit index.
When up-scaling the model from field to satellite level, the decrease in accuracy was comparable to the results from a more complex SVAT model, with a better performance again of the Apparent Thermal Inertia index especially when calculated from MODIS rather than from SEVIRI data (r^2= 0.69; MAE=13.48 Wm^{-2}). The global MODIS 8-day evapotranspiration product (MOD16) was also evaluated at the site and failed to capture the dynamics of evapotranspiration in this Sahelian savanna.

1. INTRODUCTION

Evapotranspiration (or latent heat flux expressed in energy terms, λE) represents 90% of the annual precipitation in water-limited regions which cover 40% of the Earth's surface (Glenn et al. 2007). The Sahel is located in a transitional climate region and is thus expected to be extremely sensitive to climate change ((Mougin et al. 2009a)). Improving estimates of temporal and spatial variations of λE is crucial for understanding land surface-atmosphere interactions and to improve hydrological and agricultural management (Yuan et al. 2010).
λE can be estimated at regional scales using remote sensing data. Some models rely on the Penman-Monteith (PM) combination equation and λE can be partitioned into soil and vegetation components (Leuning et al. 2008). With this approach, the challenge is to characterize the spatial and temporal variation in surface conductances (Zhang et al. 2010).
A simple way to estimate surface conductances is to use prescribed sets of parameters based on biome-type maps (Zhang et al. 2010). Other approaches perform optimization with field data but can lead to a lack of estimates over vast regions of the globe, such as the Sahel, due to the scarcity of field measurements (Yuan et al. 2010).
(Priestley and Taylor 1972) simplified the Penman-Monteith equation (PT) for equilibrium evapotranspiration over large regions by replacing the surface and aerodynamic resistance terms with an empirical multiplier α_{PT} (Zhang et al. 2009). The PT equation is theoretically less accurate than PM although uncertainties in parameter estimation using PM can results in higher errors. (Fisher et al. 2008) proposed a model based on PT to estimate monthly actual λE. The authors used biophysical constraints to reduce λE from a maximum potential value, λEp, in response to multiple stresses.
PM and PT satellite-based approaches have taken advantage of optical remote sensing data to estimate vegetation properties. However, thermal information has been incorporated in only few studies using coarse (0.25º) microwave AMSR-E data (Miralles et al. 2011) even though formulations using longwave infrared *Ts* could help to track changes in surface conductance (Berni et al. 2009); (Boegh et al. 2002), soil evaporation (Qiu et al. 2006), surface water deficit (Boulet et al., 2007; Moran et al., 1994) or soil water content (Gillies & Carlson, 1995; (Sandholt et al. 2002); Nishida et al., 2003) at spatial resolutions of 1-3 km. In relation to soil moisture, the early work of (Price 1977) and (Cracknell and Xue 1996) for mapping soil thermal inertia is now being revisited for soil moisture mapping (Cai et al. 2007; Sobrino et al. 1998; Verstraeten et al. 2006).
The general aim of this work is to develop an operational monitoring system for actual evapotranspiration in the Sahel using solely satellite and reanalyses data. We adapted a daily version of the two-source Fisher´s model with minimum requirements of climatic inputs, no field-calibration requirements and spatial resolution of 1-4 km. Fisher-daily, was evaluated at the point (flux site) level in a savanna site in the Sahel (Mali).
The specific objectives were:

- Evaluate two soil moisture parameterizations: an Apparent Thermal Inertia index and an atmospheric water deficit index.

* International Research Institute for Climate and Society
Monell 138B, 61 Route 9W
Palisades, New York 10964, NY (USA)
Phone: 845 680-4442. email: mggarcia@iri.columbia.edu

- Evaluate the performance of MODIS vs. SEVIRI as inputs for the Apparent Thermal Inertia Index
- Compare satellite model outputs with the performance of a global satellite LE product (MOD16A2)

2. DATA

2.1. Study site and Field data

The Agoufou site is an open woody savanna located at 15.34°N, 1.48°W in the Sahel (Mali). It is homogeneous over several kilometers, with trees representing less than 5% of vegetation cover. A comprehensive description of the site is provided by (Mougin et al. 2009b). The region experiences a single rainy season with most precipitation falling between late June and mid September followed by a long dry season of around 8 months (Figure 1).
In-situ data for the 2007 growing season were provided by the African Monsoon Multidisciplinary Analyses (AMMA) project. Sensible heat flux was measured with sonic anemometers (CSAT) measuring the three vector components of the wind at 20 Hz. Latent heat fluxes were measured with the eddy–covariance system (Campbell CR3000 and CSAT3–LiCor7500, Campbell Scientific Inc. Logan, UT, USA and Li–Cor Inc., Lincoln, NE, USA). The four components of the net radiation were measured with a CNR1 (Kipp and Zonen CNR1, Delft, Holland).
Measurement height for the flux sensors are 2.2 m. Soil heat fluxes were computed from soil temperature measurements. See (Timouk et al. 2009) for more details. Wind speed and direction (Vector A100R), land surface temperature (Everest 4000.4zl), air temperature and humidity (HMP 45C, Vaisala) and precipitation (Delta T, RG1) were also measured. Time domain reflectometry sensors (CampbellCS616, Campbell Scientific INC., USA) measured volumetric Soil Water Content at several depths with the shallower probe, the one used in this work, located at 5 cm.

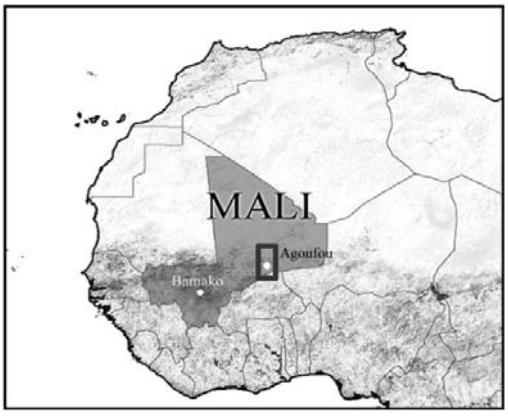

Figure 1: Study site in the Sahel (Agoufou, Mali) (15.34°N, 1.48°W), an open woody savanna instrumented within the Monsoon Multidisciplinary Analyses (AMMA) project.

The fraction of vegetation cover is 50%, with a maximum average height of 0.4 m for the herbaceous cover. A period starting prior and finishing after the rains was evaluated (DOY 170 to 315). No gap filling has been performed. Gaps in flux data are present notably in late July to early August.

2.2. Satellite and climatic data

Satellite data acquired from the MODIS sensor included: *LAI* and f_{PAR} from combined product from Terra and Acqua platforms (MCD15A3) consisting of 4-day composites of 1 km pixel. The *LAI* and f_{PAR} were assumed to be constant within the 4-day compositing period. Day and night LST (Lands Surface Temperature) and emissivity at 1 km were acquired from Terra (MOD11A1). Daily surface reflectance from Terra (MOD09GA) at 1 km was acquired to estimate albedo using a linear combination of spectral bands (Liang et al., 2001).
Land Surface Temperature (*LST*) and broadband surface albedo (α) products were developed by the Satellite Application Facility for Land Surface Analysis (Land-SAF) with data from the Spinning Enhanced Visible and Infrared Imager (SEVIRI) radiometer, onboard of the MSG (Meteosat Second Generation). The MSG-SEVIRI sensor includes 12 separate channels and 15 min temporal resolution. As for any geostationary satellite the trade-off is the low spatial resolution of 4.8 km at nadir (spatial sampling is 3 km) and large view angles (Schmetz et al. 2002). The LST algorithm is based on a generalized split window adapted to SEVIRI data (Trigo et al. 2008). The albedo product is based on shortwave channels at 0.6, 0.8 and 1.6 µm. It has an effective temporal scale of 5 days and updated on a daily basis (Geiger et al. 2008).
Incoming solar radiation, Relative Humidity (*RH*) and minimum, maximum and mean air temperature (*Tair*) were obtained from the NASA-power database from the Agroclimatology archive of 1º spatial resolution (http://power.larc.nasa.gov). For the year 2007 the solar parameters were taken from the NASA/GEWEX Surface Radiation Budget (GEWEX SRB 3.0 - http://eosweb.larc.nasa.gov/PRODOCS/srb/table_srb.html) project and the meteorological parameters are from NASA's Global Model and Assimilation Office (GMAO - http://gmao.gsfc.nasa.gov), Goddard Earth Observing System model version 4 (GEOS-4). To obtain the air temperature at the time of satellite overpass a sinusoidal function of day length, latitude and mean, minimum and maximum temperatures was used (Chapter 2, Campbell & Norman, 1998).

3. METHODOLOGY

3.1. Fisher-Daily Model Description

The daily model proposed here (hereafter Fisher-daily) is a modified version of the algorithm described in (Fisher et al. 2008) λE is partitioned into canopy transpiration (λE_c) and soil evaporation (λE_s) (equation 1).
Actual λE is calculated based on potential evapotranspiration of soil (λEp_s) and canopy (λEp_c) which are reduced from their potential level using different constraints (multipliers) based on plant physiological status and soil moisture availability (Fisher et al. 2008). λE_p was calculated using (Priestley and Taylor 1972) equation.

$$\lambda E = \lambda E_c + \lambda E_s \qquad \text{(equation 1)}$$

Three plant physiological constraints were considered to regulate evapotranspiration: green canopy fraction (f_g), a plant temperature constraint (f_T) and a plant moisture constraint (f_M) (equation 2).

$$\lambda E_c = f_g f_T f_M \lambda Ep_c \qquad \text{(equation 2)}$$

All the equations and variables are described in Table 1**.**
The soil evaporation component was constrained by a soil moisture limitation, f_{SM} (equation 3).

$$\lambda E_s = f_{SM} \lambda Ep_s \qquad \text{(equation 3)}$$

In this work, we calculated three different estimates of f_{SM} (see Table 1).The first is based on field measurements of volumetric soil water content (*SWC*) ($f_{SM\text{-}SWC}$), where *SWC* was rescaled between a minimum (SWC_{min}) and a maximum value (SWC_{Max}) (Fisher et al. 2008). In our case, SWC_{min} was estimated as the minimum value of the dry season and SWC_{Max} as the *SWC* 24 hours after a strong rainfall event, which can be considered as an estimate of the field capacity. If $SWC > SWC_{Max}$ then $f_{SM\text{-}SWC}$ =1.
The second approach to estimate f_{SM} was the original Fisher's model formulation based on the link between atmospheric water deficit and soil moisture ($f_{SM\text{-}VPD}$) (Bouchet 1963); (Morton 1983). The third f_{SM} estimate was based on the apparent thermal inertia (*ATI)* concept using *Ts* and albedo ($f_{SM\text{-}ATI}$). It was introduced by (Price 1977) and expanded by (Cracknell and Xue 1996); Sobrino et al. (1998) and (Lu et al. 2009). In this study we estimated *ATI* following Verstraeten et al. (2006) (see equation 4) relying on broadband albedo (α), and the difference between maximum daytime (Ts_{DMax}) and minimum nightime (Ts_{Dmin}) surface temperature, and a solar correction factor C that normalizes for changes in solar irradiance with latitude, and the solar declination angle. It is assumed that *ATI* reflects both soil and canopy water content if the *Ts* includes both soil and vegetation components (Verstraeten et al. 2006; (Tramutoli 2000).

$$ATI = C\frac{1-\alpha}{Ts_{DMax} - Ts_{D\,min}} \qquad \text{(equation 4)}$$

To relate remotely sensed *ATI* and soil moisture and obtain $f_{SM\text{-}ATI}$ it was assumed that the minimum and maximum seasonal *ATI* (ATI_{min} and ATI_{Max}) correspond to residual and saturated soil moisture contents following Verstraeten et al. (2006) (see equation in Table 1).

3.2. Sensitivity analysis

Sensitivity analysis was performed to evaluate the effects of uncertainty on input or parameters. Global Sensitivity Analysis (GSA) of Fisher-daily model was performed using Extended Fourier Amplitude Sensitivity Test (EFAST) (Saltelli et al. 1999). A Fourier decomposition is used to obtain the fractional contribution of the individual input factors to the variance of the model prediction (Campolongo F. 2000).
To identify the relative importance of each model input in terms of its contribution to the output variance of daily evapotranspiration, perturbations for each variable were applied around the mean value of the growing season and also around mean monthly values. *Rn, G, NDVI* and *Tair* were varied by ±10% around their monthly means and annual mean based on uncertainty of measurements. For the constant model parameters: m_1, b_1, m_2, b_2, k_{Rn}, and k_{PAR}, the range of uncertainty was based on values used in the literature **(**Table 2**)**. A perturbation of ±25% around the mean was considered for the soil moisture constraint (f_{SM}) and the plant temperature constraint (f_T).

Table 1: Equations and variables involved in estimating Fisher-daily model biophysical constraints, plant variables and energy variables. f_{APAR} is the fraction of Absorbed Photosynthetically Active Radiation, f_{IPAR} the fraction of intercepted photosynthetically active radiation, T_{opt} is optimum temperature for plant growth (25 °C), Ta_m (daily mean air temperature (°C), $f_{APARMAX}$ is maximum f_{APAR}, SWC , Soil Water Content (m^3m^{-3}), RH is relative humidity (%), VPD is the vapor pressure deficit (kPa), Ts is daily average radiometric surface temperature, Ts_{min} is the seasonal minimum Ts, Ts_{MAX} is the seasonal maximum Ts. ATI is the apparent thermal inertia index ($°C^{-1}$), Rn is daily net radiation (Wm^{-2}). Values for parameters: k_{Rn}=0.6 (Impens and Lemeur 1969); k_{PAR}=0.5 (Brownsey et al. 1976); m_1=1.16; b_1=-0.14; (Myneni and Williams 1994); m_2=1.0; $b_{2=}$=-0.05 (Fisher et al. 2008), γ (psychrometric constant)= 0.066 $kPaC^{-1}$; β=1kPa, α_{PT} =1.26 Priestley -Taylor coefficient; Δ is the slope of the saturation-to-vapor pressure curve (PaK^{-1}).

	Variable	Description	Equation	Reference
Biophysical constraints	f_g	Green canopy fraction	$fg = \frac{f_{APAR}}{f_{IPAR}}$	(Fisher et al. 2008)
	f_T	Plant temperature constraint	$f_T = 1.1814 \cdot \left[1+e^{0.2\cdot(T_{opt}-10-Ta_m}\right]^{-1} \cdot \left[1+e^{0.3(-T_{opt}-10-Ta_m}\right]^{-1}$	(Potter et al. 1993)
	f_M	Plant moisture constraint	$f_M = \frac{f_{APAR}}{f_{APARMax}}$	(Fisher et al. 2008)
	f_{SM}	Soil moisture constraint	• $f_{SM\text{-}SWC} = 1-\left(\frac{SWC-SWC_{min}}{SWC_{Max}-SWC_{min}}\right)$	(Fisher et al. 2008)
			• $f_{SM-Fisher} = RH^{VPD/\beta}$	(Fisher et al. 2008)
			• $f_{SM-ATI} = \left(\frac{ATI-ATI_{min}}{ATI_{Max}-ATI_{min}}\right)$	This study
Plant variables	f_{APAR}	*PAR* fraction absorbed by green vegetation	$f_{APAR-MODIS}$	(Myneni et al. 2002)
	f_{IPAR}	*PAR* fraction intercepted by total vegetation	$f_{IPAR} = m_2 \cdot NDVI + b_2$	(Fisher et al. 2008)
	f_c	fractional vegetation cover	$fc = f_{IPAR}$	(Campbell JS (1998))
	LAI	Leaf Area Index	LAI_{MOD15}	(Myneni et al. 2002)
Energy variables	Rn_s	Net radiation to the soil	$Rn_s = Rn \cdot e^{(-k_{Rn}LAI)}$	(Ross, 1976) (Norman et al. 1995)
	λEp_c	Priestley-Taylor potential evapotranspiration for canopy	$\lambda Ep_c = \alpha_{PT}\frac{\Delta}{\Delta+\gamma}(Rn-Rn_s)$	(Norman et al. 1995)
	λEp_s	Priestley-Taylor potential evapotranspiration for soil	$\lambda Ep_s = \alpha_{PT}\frac{\Delta}{\Delta+\gamma}(Rn_s-G)$	(Norman et al. 1995)

Table 2: Ranges of variation for input parameters and variables in Fisher-daily model. For *Rn*, *G*, *NDVI* and T_{air} ranges of ± 10% around monthly means and annual mean was considered. For the constant model parameters: m_1, b_1, m_2, b_2, k_{Rn}, and k_{PAR}, the range of uncertainty was based on values used in the literature. For the soil moisture constraint (f_{SM}) and the plant temperature constraint (f_T) a range of ± 25% around the mean was considered.

Input var	Range	Reference
T_{air}	±10% of mean	This study
Rn	±10% of mean	This study
G	±10% of mean	This study
f_T	±25% of mean	This study
f_{SM}	±25% of mean	This study
NDVI	±10% of mean	This study
m_1	[1.16, 1.42]	This study
b_1	[-0.039, -0.025]	This study
m_2	[0.9, 1.2]	(Fisher et al. 2008)
b_2	[-0.06, -0.04]	Fisher et al. (2008)
k_{Rn}	[0.3, 0.6]	Ross (1976)
k_{PAR}	[0.3, 0.6]	Ross (1976)

3.3. Evaluation of soil moisture constraints using field and satellite data

We evaluated which of the three parameterizations of the soil moisture constraint to soil evaporation (see Table 1) produced better results using different input data. First, the model was run with field measurements for *Rn* and *Tair*. The soil moisture constraint calculated from field data, $f_{SM\ -SWC,}$ was used as a benchmark as it should provide the more accurate results. The two soil moisture constraints: $f_{SM\ -VPD}$ and $f_{SM\ -ATI}$ were first calculated using inputs from field measurements. Also it was tested the change in accuracy when using $f_{SM\ -ATI}$ from satellite MSG. The different model versions are summarized in Table 3.

In a second step, the model was run using solely satellite and climatic reanalyses products. Thus, forcing data from NASA-Power for *Rn* and *Tair* were used and the soil moisture constraints for $f_{SM\ -VPD}$ and $f_{SM\ -ATI}$ were calculated exclusively from satellite and reanalyses data (see Table 3). In this step we evaluated the differences when calculating $f_{SM\ -ATI}$ from MODIS and from SEVIRI data.

Instantaneous *Rn* from satellite data was estimated by calculating the shortwave and longwave components as described in (Garcia et al. 2007). To estimate daily *Rn* from instantaneous *Rn*, a sinusoidal function based on day-length was used (Jackson et al., 1983).

Model results were compared with λE from Eddy Covariance fluxes and the coefficient of determination (r^2), Mean Average Error (MAE), the bias, the RMSE (Root Mean Square Error) and MPE (Mean Absolute Percentage Error) were used as indicators of model performance. To compare modeled λE with λE measurements from Eddy we forced the closure of the equation for energy balance considering the criteria of preserving the Bowen ratio (Twine et al. 2000).

Table 3: Seven versions of Fisher-daily differing in (a) the forcing variables *Rn* and *Tair* being from in-situ or from satellite data (b) the formulation for the soil moisture constraint: $f_{SM\text{-}SWC}$ (from measured volumetric soil water content), $f_{SM\text{-}VPD}$ (from atmospheric water deficit), and $f_{SM\text{-}ATI}$ (from apparent thermal inertia) and (c) the input data for the soil moisture constraints obtained from in-situ or satellite (MSG or MODIS data).

Forcing	Nr	Model name	f_{SM}/data	*Rn, Tair*
Field	1	Field-SWC	*SWC/in situ*	In situ
	2	Field-VPD	*VPD/in situ*	In situ
	3	Field-ATI in situ	*ATI/in situ*	In situ
	4	Field-ATI MSG	*ATI/MSG*	In situ
Satellite	5	Satellite-VPD	*VPD/NASA Power*	NASA-Power
	6	Satellite-ATI MSG	*ATI/MSG*	NASA-Power
	7	Satellite-ATI MODIS	*ATI/MODIS*	NASA-Power

3.4. Comparison of model satellite outputs with the global MODIS (MOD16) evapotranspiration product

Finally, model satellite outputs were compared to the global MODIS evapotranspiration product (MOD16) developed by Mu et al., (2011; 2007). Daily model estimates and eddy covariance λE measurements were aggregated at 8-day time scale considering only clear-sky days in order to compare with the MOD16 product at the same time-step. Only MOD16 data passing quality checks (flags) were considered for model evaluation. The results were converted from Wm^{-2} into $mmday^{-1}$ to match the units of MOD16.

4. RESULTS

4.1. Sensitivity analysis

Considering the variability around mean annual conditions, the contribution to uncertainty was less than 20% for most parameters. The greatest uncertainty was due to two of the biophysical constraints: f_{SM} and f_T with 22.19% and 17.68 % respectively (total effect). Five other variables involved in *LAI* estimation and energy partition between soil and canopy contributed around 12% to model uncertainty (Figure 2).

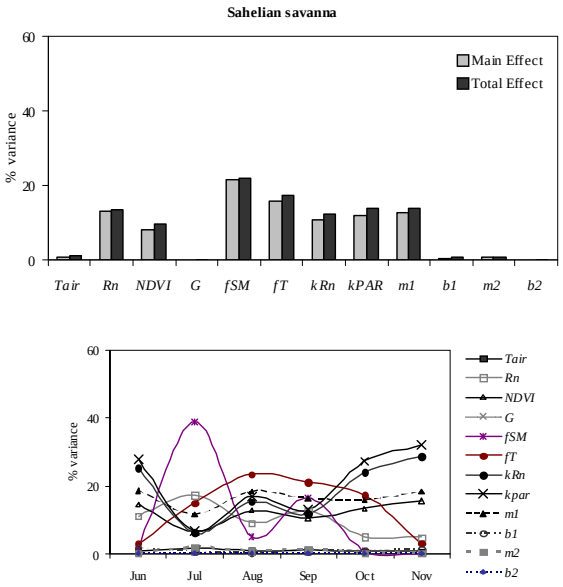

Figure 2. Upper panel: sensitivity of modeled evapotranspiration according to mean annual conditions (% percentage of explained variance). Main effect is the variance explained without considering interactions among variables and total effect considering interactions. Lower panel: sensitivity of modeled evapotranspiration considering monthly (total effect). Uncertainty levels were set as ±10% of the mean for input variables *NDVI*, Ta_m, *Rn*, and *G* and of ±25% of the mean for the soil moisture (f_{SM}) and plant temperature (f_T) constraints. For constant model parameters: m_1, b_1, m_2, b_2, k_{Rn}, and k_{PAR}, the range of uncertainty was based on values used in the literature.

However, the relative importance of each variable depends on the time of the year. At the beginning of the season, λE was most sensitive to accuracy in f_{SM} reaching the maximum value of explained variance among all variables and months (40%). During the maximum peak of *NDVI*, in the middle of the season, the greatest sensitivity was due to f_T, and m_1 (involved in f_M and f_g estimates via f_{APAR}). During the senescent phase, the model was more sensitive to accuracy in k_{PAR} and k_{Rn}, involved in energy partition into soil and vegetation.

4.2. Evaluation of soil moisture parameterizations using field and satellite data

Figure 3 shows the changes in the accuracy of λE retrievals from using different soil moisture parameterizations. Using measured *SWC* the model λE explains up to 86% of the variance, which considering that the closure error of the eddy covariance data represents 5.78% of the available energy (*Rn*-*G*) at daily scale is also close to the instrumental accuracy. However, in this site during the growing season there was a systematic underestimate of λE during the period of maximum growth followed by an overestimate. When using the atmospheric water deficit index correlations were well below those found for $f_{SM\text{-}SWC}$ (r^2=0.61) and with high biases around 25 Wm^{-2}. Regarding the thermal Inertia soil moisture constraint $f_{SM\text{-}ATI}$, using in-situ data, model performance was practically equivalent to that using *SWC* ($f_{SM\text{-}SWC}$), with $r^{2\text{-}}$=0.83 and slightly higher errors but similar or lower biases. When running the model using satellite MSG instead of in-situ data for $f_{SM\text{-}ATI}$, good results were obtained for r^2 =0.80 and MAE=20.21 Wm^{-2} but higher biases than with in-situe data were detected due to λE underestimates during the growing season. This was due to the fact that the diurnal *Ts* difference (TsDMax-TsDmin) was always higher for MSG than for in-situ data producing lower soil moisture (f_{SM}) values.

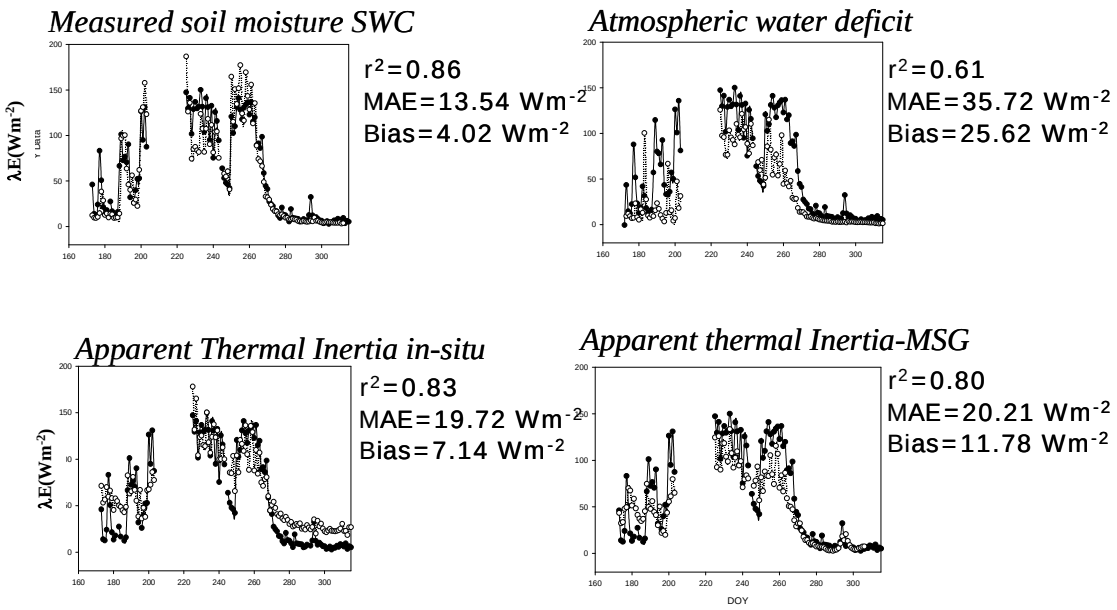

Figure 3: Daily λE (Wm^{-2}) in Agoufou (Mali) from Eddy Covariance data (black dots) and modeled (white dots) during 2007. The model was run using different soil moisture constraints: $f_{SM\text{-}SWC}$ from measured volumetric soil water, $f_{SM\text{-}VPD}$ from atmospheric water deficit, $f_{SM\text{-}ATIin\text{-}situ}$ from apparent thermal inertia from in-situ measurements and $f_{SM\text{-}ATI\text{-}MSG}$ from apparent thermal inertia from MSG-SEVIRI measurements. In model versions *Rn* and *Tair* were from in-situ measurements.

We evaluated the sensitivity of $f_{SM\text{-}VPD}$ to b values between 0.05 to 2, and to the use of daily average or midday conditions for *RH* and *VPD*. Table 4 shows the results for the two levels of b that provided the best results: b=0.1 kPa, that was applied at a global scale by in (Mu et al., 2007), and b=1 kPa applied in (Fisher et al., 2008). The best results corresponded to b=1 kPa and daily average conditions which are the parameters subsequently used for the satellite model estimates instead of the midday original conditions.

Table 4: Evaluation of Fisher-daily λE with Eddy Covariance data for different parameterizations of the soil moisture constraint derived from atmospheric water deficit. Results are shown for midday and daily average conditions for *RH* (relative humidity) and *VPD* (Vapor Pressure Deficit) and for β=0.1 kPa and β=1 kPa.

Condt	β (kPa)	r^2	MAE	bias	RMSE	MPE (%)
daily	1	0.80	18.08	8.47	24.35	29.0
	0.1	0.66	23.60	37.92	49.94	37.9
Mid-day	1	0.61	35.72	25.62	40.61	57.3
	0.1	0.65	21.86	39.71	52.45	35.1

Figure 4 compares three model versions based only on satellite and reanalyses input data with eddy covariance λE. The correlations were lower with respect to those obtained when using in-situ *Rn* and *Tair* especially for the case of the $f_{SM\text{-}ATI}$ index, which showed the highest biases when using SEVIRI data of around 20 Wm^{-2}. This is due to a bias in the *Rn* estimates from SEVIRI that needs to be corrected in future algorithm versions.

Although the use of MODIS data resulted in a lower amount of observations (N=33 vs. N=66) compared to SEVIRI, as there is only a day and a night overpass, the results were more accurate and with a lower bias.

Despite of the decrease in accuracy compared to in-situ modeling (Figure 3), results aggregated at daily-time scale were similar to those from a SVAT model based on Shuttleworth and Wallace dual coupled to an hydrological model run with the same dataset and using a higher number of parameters (Ridler et al., 2012). The SVAT model assimilated LST from the MSG-SEVIRI sensor and soil moisture from the Advanced Microwave Scanning Radiometer on the Earth (AMSR–E) resulting in r^2=0.63 and MAE=39.24 Wm^{-2} compared with field data and producing also underestimates in λE but a higher number of observations were available.

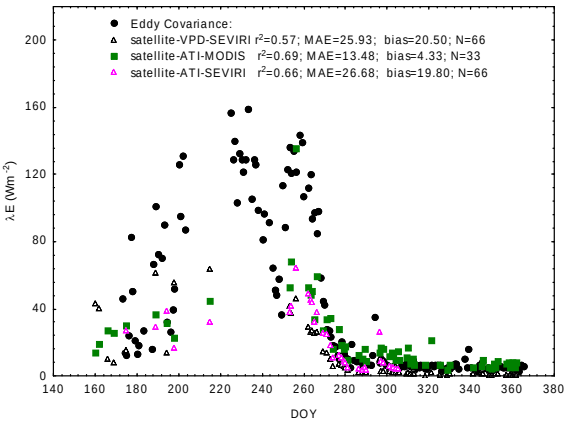

Figure 4: Daily λE (Wm^{-2}) in Agoufou (Mali) from Eddy Covariance data (black dots) and model results using solely satellite information. The model was run using $f_{SM\text{-}VPD}$ from atmospheric water deficit, and $f_{SM\text{-}ATI}$ from apparent thermal inertia calculated alternatively with MSG-SEVIRI or MODIS data. Statistics comparing models with eddy covariance data are shown in the chart, r^2 is the coefficient of determination, MAE is the Mean Absolute error, bias is the difference between observed (in Wm^{-2}) and model, and N is the number of observations.

4.3. Comparison of model satellite outputs with the MODIS (MOD16) evapotranspiration product

When aggregating at 8-day time-step the satellite model results, the accuracy improved with respect to daily time-step with r^2 between 0.70-0.80 depending on the soil moisture constraint used with better results for Apparent Thermal Inertia than for the atmospheric water deficit approach. The best results corresponded to the use of the Thermal Inertia index (ATI) derived from MODIS data (Figure 5). However, the MOD16 ET product failed to capture the dynamics of evapotranspiration in this ecosystem with most of the model estimates disregarded due to quality flags and failure to capture the senescence process.

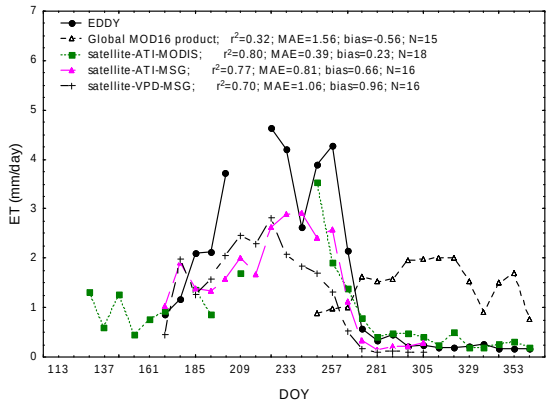

Figure 5: 8-day *ET* (mm/day) in Agoufou (Mali) from Eddy Covariance data (black dots), the global MOD16 ET product, and three model versions relying only on satellite information: satellite-VPD-MSG was run using $f_{SM\text{-}VPD}$ from atmospheric water deficit, satellite-ATI-MSG used $f_{SM\text{-}ATI}$ calculated with MSG-SEVIRI and satellite-ATI-MODIS used $f_{SM\text{-}ATI}$ calculated with MODIS data. Statistics comparing models with eddy covariance data are shown in the chart, r^2 is the coefficient of determination, MAE is the Mean Absolute error, bias is the difference between observed and model (in mm/day), and N is the number of observations.

5. CONCLUSIONS

In dryland regions one of the most critical parameters constraining evapotranspiration is soil moisture. An evapotranspiration model based on the Priestley-Taylor equation depressed according to multiple stress factors, Fisher-daily, was evaluated in a savanna site in the Sahel (Mali). The model was successful to estimate evapotranspiration at the field level, with a better performance of the model when using a soil moisture constraint based on the Thermal Inertia index (r^2=0.83; MAE=19.2 Wm^{-2}) than with an atmospheric water deficit index.

When up-scaling the model from field to satellite level, the decrease in accuracy was comparable to that observed when using a more complex SVAT model with data assimilation, with a better performance again of the Apparent Thermal Inertia index (r^2= 0.69; MAE=13.48 Wm^{-2}) over the atmospheric water deficit index.

Regarding the satellite data used to estimate the Apparent Thermal Inertia index, MODIS provided more accurate results than SEVIRI data but fewer observations were available due to its lower frequency of acquisition.

The global MODIS 8-day evapotranspiration product (MOD16) failed to capture the dynamics of evapotranspiration in this Sahelian savanna, while our satellite models improved their accuracy at 8-day time scale compared to daily time-step being able to detect the onset and the end of the rainy season as well as stress features despite of the biases.

Future work should focus on bias correction and interpolation between cloudy days. Model intercomparisons with the same climatic forcings are desirable for comparison of the MOD16 and our version of the Fisher-daily model as well.

The version proposed here of the Fisher model using a soil moisture constraint based on apparent thermal inertia, $f_{SM\text{-}ATI}$ offers great potential for regionalization in the Sahel region as no field-calibrations are required and water vapor deficit estimates, required in the original version, are not necessary, being air temperature and incoming solar radiation the only input variables required, apart from routinely available satellite products.

Acknowledgements

This study was funded by the Danish Council for Independent Research and Technology and Production Sciences (FTP) Grant 09-070382. MODIS data were obtained through the online Data Pool at the NASA Land Processes Distributed Active Archive Center (LP DAAC), USGS/Earth Resources Observation and Science Center, Sioux Falls, South Dakota (http://lpdaac.usgs.gov/get_data). The authors would like to thank EUMETSAT for providing the MSG-SEVIRI data. Field data for the savanna site in Mali were collected within the frame of the AMMA project (www.amma-eu.org). The Malian site belongs to the AMMA-CATCH observatory (www.amma-catch.org). The authors acknowledge helpful comments and feedback from Rado Gucinski, Mads Olander Rasmussen, Hector Nieto and Simon Proud.

6. REFERENCES

Berni, J.A.J., Zarco-Tejada, P.J., Sepulcre-Canto, G., Fereres, E., & Villalobos, F. (2009). Mapping canopy conductance and CWSI in olive orchards using high resolution thermal remote sensing imagery. *Remote Sensing of Environment, 113*, 2380-2388

Boegh, E., Soegaard, H., & Thomsen, A. (2002). Evaluating evapotranspiration rates and surface conditions using Landsat TM to estimate atmospheric resistance and surface resistance. *Remote Sensing of Environment, 79*, 329-343

Bouchet, R.J. (1963). Evapotranspiration reelle et potentielle, signification climatique. *International Association of Hydrological Sciences (IAHS), Pub., 62*, 134–142

Brownsey, G.J., Eldridge, J.W., Jarvis, D.A., Ross, G., & Sanders, I. (1976). New Light-Scattering Photogoniometer for Accurate Measurements. *Journal of Physics E-Scientific Instruments, 9*, 654-658

Cai, G., Xue, Y., Hu, Y., Wang, Y., Guo, J., Luo, Y., Wu, C., Zhong, S., & Qi, S. (2007). Soil moisture retrieval from MODIS data in Northern China Plain using thermal inertia model. *International Journal of Remote Sensing, 28*, 3567-3581

Campbell JS, N.J. ((1998)). *An Introduction to Environmental Biophysics*, : Springer.

Campolongo F., S.A., Sørensen, T., Tarantola S. (2000). Hitchhiker's guide to sensitivity analysis. *Sensitivity analysis*, (pp. 15-47): Wiley, New York

Cracknell, A.P., & Xue, Y. (1996). Thermal inertia determination from space - A tutorial review. *International Journal of Remote Sensing, 17*, 431-461

Fisher, J.B., Tu, K.P., & Baldocchi, D.D. (2008). Global estimates of the land–atmosphere water flux based on monthly AVHRR and ISLSCP-II data, validated at 16 FLUXNET sites. *Remote Sensing of Environment, 112*, 901-919

Garcia, M., Villagarcia, L., Contreras, S., Domingo, F., & Puigdefabregas, J. (2007). Comparison of three operative models for estimating the surface water deficit using ASTER reflective and thermal data. *Sensors, 7*, 860-883

Geiger, B., Carrer, D., Franchisteguy, L., Roujean, J.L., & Meurey, C. (2008). Land Surface Albedo Derived on a Daily Basis From Meteosat Second Generation Observations. *Ieee Transactions on Geoscience and Remote Sensing, 46*, 3841-3856

Glenn, E.P., Huete, A.R., Nagler, P.L., Hirschboeck, K.K., & Brown, P. (2007). Integrating Remote Sensing and Ground Methods to Estimate Evapotranspiration. *Critical Reviews in Plant Sciences, 26*, 139-168

Impens, I., & Lemeur, R. (1969). Extinction of net radiation in different crop canopies. *Archiv für Meteorologie, Geophysik und Bioklimatologie Serie B, 17*, 403-412

Leuning, R., Zhang, Y.Q., Rajaud, A., Cleugh, H., & Tu, K. (2008). A simple surface conductance model to estimate regional evaporation using MODIS leaf area index and the Penman-Monteith equation. *Water Resources Research, 44*

Lu, S., Ju, Z., Ren, T., & Horton, R. (2009). A general approach to estimate soil water content from thermal inertia. *Agricultural and Forest Meteorology, 149*, 1693-1698

Miralles, D.G., Holmes, T.R.H., De Jeu, R.A.M., Gash, J.H., Meesters, A.G.C.A., & Dolman, A.J. (2011). Global land-surface evaporation estimated from satellite-based observations. *Hydrology and Earth System Sciences, 15*, 453-469

Morton, F.I. (1983). Operational estimates of areal evapotranspiration and their significance to the science and practice of hydrology. *Journal of Hydrology, 66*, 1-76

Mougin, E., Hiernaux, P., Kergoat, L., Grippa, M., de Rosnay, P., Timouk, F., Le Dantec, V., Demarez, V., Lavenu, F., & Arjounin, M. (2009a). The AMMA-CATCH Gourma observatory site in Mali: Relating climatic variations to changes in vegetation, surface hydrology, fluxes and natural resources. *Journal of Hydrology, 375*, 14-33

Mougin, E., Hiernaux, P., Kergoat, L., Grippa, M., de Rosnay, P., Timouk, F., Le Dantec, V., Demarez, V., Lavenu, F., Arjounin, M., Lebel, T., Soumaguel, N., Ceschia, E., Mougenot, B., Baup, F., Frappart, F., Frison, P.L., Gardelle, J., Gruhier, C., Jarlan, L., Mangiarotti, S., Sanou, B., Tracol, Y., Guichard, F., Trichon, V., Diarra, L., Soumaré, A., Koité, M., Dembélé, F., Lloyd, C., Hanan, N.P., Damesin, C., Delon, C., Serça, D., Galy-Lacaux, C., Seghieri, J., Becerra, S., Dia, H., Gangneron, F., & Mazzega, P. (2009b). The AMMA-CATCH Gourma observatory site in Mali: Relating climatic variations to changes in vegetation, surface hydrology, fluxes and natural resources. *Journal of Hydrology, 375*, 14-33

Myneni, R.B., Hoffman, S., Knyazikhin, Y., Privette, J.L., Glassy, J., Tian, Y., Wang, Y., Song, X., Zhang, Y., Smith, G.R., Lotsch, A., Friedl, M., Morisette, J.T., Votava, P., Nemani, R.R., & Running, S.W. (2002). Global products of vegetation leaf area and fraction absorbed PAR from year one of MODIS data. *Remote Sensing of Environment, 83*, 214-231

Myneni, R.B., & Williams, D.L. (1994). On the Relationship between Fapar and Ndvi. *Remote Sensing of Environment, 49*, 200-211

Norman, J.M., Kustas, W.P., & Humes, K.S. (1995). Source Approach for Estimating Soil and Vegetation Energy Fluxes in Observations of Directional Radiometric Surface-Temperature. *Agricultural and Forest Meteorology, 77*, 263-293

Potter, C.S., Randerson, J.T., Field, C.B., Matson, P.A., Vitousek, P.M., Mooney, H.A., & Klooster, S.A. (1993). Terrestrial Ecosystem Production - a Process Model-Based on Global Satellite and Surface Data. *Global Biogeochemical Cycles, 7*, 811-841

Price, J.C. (1977). THERMAL INERTIA MAPPING: A NEW VIEW OF THE EARTH. *J Geophys Res, 82*, 2582-2590

Priestley, C.H.B., & Taylor, R.J. (1972). On the Assessment of Surface Heat Flux and Evaporation Using Large-Scale Parameters. *Monthly Weather Review, 100*, 81-92

Qiu, G.Y., Shi, P.J., & Wang, L.M. (2006). Theoretical analysis of a remotely measurable soil evaporation transfer coefficient. *Remote Sensing of Environment, 101*, 390-398

Saltelli, A., Tarantola, S., & Chan, K.P.S. (1999). A quantitative model-independent method for global sensitivity analysis of model output. *Technometrics, 41*, 39-56

Sandholt, I., Rasmussen, K., & Andersen, J. (2002). A simple interpretation of the surface temperature/vegetation index space for assessment of surface moisture status. *Remote Sensing of Environment, 79*, 213-224

Schmetz, J., Pili, P., Tjemkes, S., Just, D., Kerkmann, J., Rota, S., & Ratier, A. (2002). An introduction to Meteosat Second Generation (MSG). *Bulletin of the American Meteorological Society, 83*, 977-+

Sobrino, J.A., El Kharraz, M.H., Cuenca, J., & Raissouni, N. (1998). Thermal inertia mapping from NOAA-AVHRR data. *Synergistic Use of Multisensor Data for Land Processes, 22*, 655-667

Timouk, F., Kergoat, L., Mougin, E., Lloyd, C.R., Ceschia, E., Cohard, J.M., Rosnay, P.d., Hiernaux, P., Demarez, V., & Taylor, C.M. (2009). Response of surface energy balance to water regime and vegetation development in a Sahelian landscape. *Journal of Hydrology, 375*, 178-189

Tramutoli, V., P. Claps, M. Marella, N. Pergola, C. Sileo (2000). Feasibility of hydrological application of thermal inertia from remote sensing. In, *2nd Plinius Conference on Mediterranean Storms,16–18* Siena, Italy,

Trigo, I.F., Peres, L.F., DaCarnara, C.C., & Freitas, S.C. (2008). Thermal land surface emissivity retrieved from SEVIRI/meteosat. *Ieee Transactions on Geoscience and Remote Sensing, 46*, 307-315

Twine, T.E., Kustas, W.P., Norman, J.M., Cook, D.R., Houser, P.R., Meyers, T.P., Prueger, J.H., Starks, P.J., & Wesely, M.L. (2000). Correcting eddy-covariance flux underestimates over a grassland. *Agricultural and Forest Meteorology, 103*, 279-300

Verstraeten, W.W., Veroustraete, F., van der Sande, C.J., Grootaers, I., & Feyen, J. (2006). Soil moisture retrieval using thermal inertia, determined with visible and thermal spaceborne data, validated for European forests. *Remote Sensing of Environment, 101*, 299-314

Yuan, W.P., Liu, S.G., Yu, G.R., Bonnefond, J.M., Chen, J.Q., Davis, K., Desai, A.R., Goldstein, A.H., Gianelle, D., Rossi, F., Suyker, A.E., & Verma, S.B. (2010). Global estimates of evapotranspiration and gross primary production based on MODIS and global meteorology data. *Remote Sensing of Environment, 114*, 1416-1431

Zhang, K., Kimball, J.S., Mu, Q., Jones, L.A., Goetz, S.J., & Running, S.W. (2009). Satellite based analysis of northern ET trends and associated changes in the regional water balance from 1983 to 2005. *Journal of Hydrology, 379*, 92-110

Zhang, Y., Leuning, R., Hutley, L.B., Beringer, J., McHugh, I., & Walker, J.P. (2010). Using long-term water balances to parameterize surface conductances and calculate evaporation at 0.05° spatial resolution. *Water Resources Research, 46*